



# Tunable Properties of Optical Selective Filters Based on One-Dimensional Plasma Superconductor Photonic Crystal

Chouaib Chettah<sup>1,2</sup> · Ouarda Barkat<sup>3</sup> · Abdelhafidh Chaabi<sup>4</sup>

Received: 18 March 2021 / Accepted: 12 April 2021 / Published online: 25 April 2021

© The Author(s), under exclusive licence to Springer Science+Business Media, LLC, part of Springer Nature 2021

## Abstract

In this paper, a new design and analysis of tunable optical selective filters containing one-dimensional photonic crystal (1D-PC), magnetized cold plasma, and superconducting materials are investigated using transfer matrix method. The effects of defective layers on transmission spectrum, the cutoff frequency, and the peak position are investigated as the function of the magnetic field and the thickness of the superconductor layer. It is found that the peak frequencies and the cutoff frequencies are affected significantly by the magnetic field applied and number of defectives layers. Also, it is demonstrated that the superconductor layer has a significant effect on the transmission spectrum. Results obtained confirmed that it is possible to make a model of a highly selective tunable filter using photonic one-dimensional plasma superconductor photonic crystal.

**Keywords** Transmission · Photonic crystals · Magnetized cold plasma · Superconductor · Photonic band gap · Defectives layers

## 1 Introduction

In recent years, the one-dimensional photonic crystals are one of the parameters that have a great effect on the performance of several applications in modern photonic technology, such as optical sensors and selective filters [1–6]. The selective filters are very promising systems for applications in the field of telecommunications such as

wavelength division multiplexing (WDM) networks and communication systems [7]. Furthermore, the use of superconductor and plasma materials in one-dimensional photonic crystals aimed at improving the performance and reducing size of these filters.

Recently, filters made of superconducting materials have attracted more attention due to two main advantages over the ordinary material. The extremely low surface resistance of superconductors facilitates the development of optical devices with better performance than conventional devices. The second is that the dielectric function of the superconductor mainly depends on the London penetration depth, which is also a function of the external temperature and the external magnetic field [8–11].

The advances on the plasma photonic crystals technology have been encouraged, in realization of optical filter [12–16]. They are artificially periodic array composed of alternating thin unmagnetized or magnetized plasmas and dielectric materials. It is well known that no magnetized plasma can be characterized by a complex frequency-dependent permittivity medium. If external magnetic field is introduced to the plasma photonic crystals and at low temperature, a new kind of plasma photonic crystals named magnetized cold plasma photonic crystals (MCP-PCs) can be obtained [17–20]. The MCP-PCs have gained a lot of attention due to their unique EM properties such as the ease of use of the external magnetic field, their magneto-optical effects based on the properties of PBGs, and

---

✉ Chouaib Chettah  
chettah\_chouaib@yahoo.fr; c.chettah@univ-skikda.dz

Ouarda Barkat  
barkatwarda@yahoo.fr

Abdelhafidh Chaabi  
ibaach@yahoo.fr

<sup>1</sup> Department of Petrochemical and Process Engineering, University 20 August 1955, Skikda, Algeria

<sup>2</sup> Hyperfrequency and Semiconductor Laboratory, University Frères Mentouri Constantine 1, Constantine, Algeria

<sup>3</sup> Department of Electronics, Electromagnetism and Telecommunications Laboratory, University Frères Mentouri Constantine 1, Constantine, Algeria

<sup>4</sup> Department of Electronics, Hyperfrequency and Semiconductor Laboratory, University Frères Mentouri Constantine 1, Constantine, Algeria

the ability to control plasma electron density. Several studies suggest that MCP-PCs are emerging as new hotspots in photon engineering due to better external magnetic field control over PBGs. In this context, we have designed an optical selective filters based on one-dimensional plasma superconductor photonic crystal.

The transfer matrix method (TMM) is employed to calculate the effects of the magnetic field and the thickness of the superconductor layer, on the width of the photonic band gaps (PBGs) and position peak. By introducing a defective layer into the (1D-PC) structure, it would be possible to generate very narrow defect modes inside a band gap; the number of these defect modes is associated with the number of defect layers.

The considered structures are  $(\text{Air}/(\text{PS})^7 \text{D}_1 (\text{PS})^7/\text{Air})$ ,  $(\text{Air}/(\text{PS})^7 \text{D}_2\text{SD}_1 (\text{PS})^7/\text{Air})$ , and  $(\text{Air}/(\text{PS})^7 \text{D}_1\text{PD}_1\text{SD}_1 (\text{PS})^7/\text{Air})$ , in which both layers  $\text{D}_1$  and  $\text{D}_2$  are dielectrics and (PS) is MCP-superconductor bi-layers. Several simulation scenarios using MATLAB will be given to show the performance of this approach. The accuracy of the analysis is approved by comparison of the computed results with real experimental measurement published data.

### 2 Problem Formulation

Consider a one-dimensional photonic crystal structure (1D-PC), which is a periodic structure composed of a multilayer stack. This structure is asymmetric in the form  $(\text{PS})^N$  immersed in free space, shown in Fig. 1. There are  $N$  stacks where each  $N/2$  period or stack is composed of a magnetized cold plasma layer (MCP) indexed  $P$  and superconductor layer indexed  $S$ . Each layer has a thickness  $d_l$  and refractive index  $n_l$ . In order to find the formulation of the structure, we assumed that in the incident electromagnetic wave from air to the plasma and superconductor layer, the layers are on the  $x$ - $y$  plane, and the  $z$  direction is normal to layer interface.

The refractive index profile of magnetized cold plasma  $P$  and superconducting  $S$  mediums can be given as:

$$\begin{cases} n_1 = n_P = \sqrt{\epsilon_P} & 0 < z < d_1 \\ n_2 = n_S = \sqrt{\epsilon_S} & d_1 < z < d_2 \end{cases} \quad (1)$$

where  $\epsilon_P, \epsilon_S, n_P, n_S, d_1$ , and  $d_2$  denote, respectively, the relative permittivity, refractive indices, and thicknesses of  $P$  and  $S$  mediums.

From the two fluid models, the complex permittivity of MCP layer  $P$  is a function of frequency  $\omega$  and static magnetic field  $\tilde{B}$  and can be expressed as [21]:

$$\epsilon_P(\omega) = 1 - \frac{\omega_{pe}^2}{\omega^2 \left( 1 - i \frac{\gamma}{\omega} \pm \frac{\omega_{le}}{\omega} \right)} \quad (2)$$

where  $\omega, \gamma, \omega_{pe}$ , and  $\omega_{le}$  are the angular frequency, the effective collision frequency, plasma, and gyro-frequency, respectively.  $\omega_{pe}$  and  $\omega_{le}$  are given by:

$$\omega_{pe} = \sqrt{n_e e^2 / m \epsilon_0} \quad (3)$$

and

$$\omega_{le} = e\tilde{B}/m \quad (4)$$

where  $e, m, n_e$ , and  $\epsilon_0$  are the electronic charge, the electronic mass, the electron density, and the free-space permittivity, respectively.

In Eq. (2), the sign ( $\pm$ ) in  $\omega_{le}$  corresponds to the application of a positive or negative external magnetic field; in other words, the static magnetic field is applied in a  $d^+z$  or  $d^-z$  direction [21].

The refractive index of the superconductor layer  $P$  is:

$$n_{\text{Super}} = \sqrt{\epsilon_S} = \sqrt{1 - (\omega_{th}/\omega)^2} \quad (5)$$

where  $\omega_{th}$  is the threshold frequency of the superconductor given by [22–25]:

$$\omega_{th}^2 = \frac{1}{\mu_0 \epsilon_0 \lambda_L^2} \quad (6)$$

where  $\lambda_L$  is the temperature-dependent London penetration depth given by:

Fig. 1 Structure of the one-dimensional MCP-superconductor photonic crystal

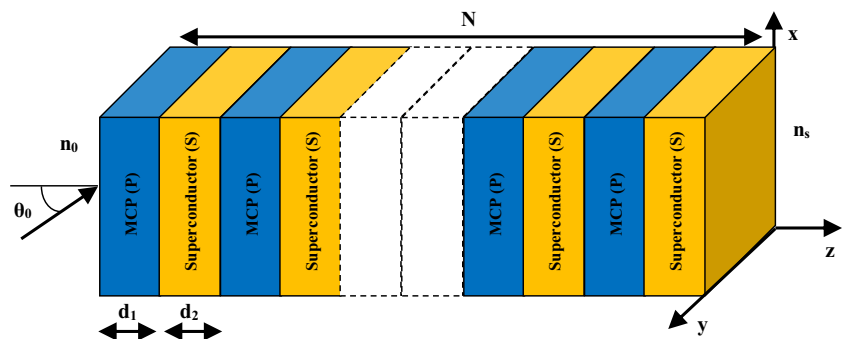
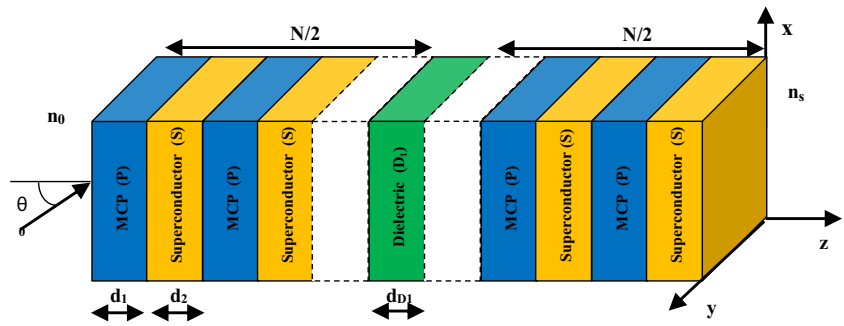


**Fig. 2** Schematic representation of the 1D-PC MCP-superconductor defected by dielectric material



$$\lambda_L^2 = \frac{\lambda_0^2}{1 - \left(\frac{T}{T_C}\right)^4} \tag{7}$$

where  $\lambda_0$  is the penetration depth at  $T = 0$  K and  $T$  and  $T_C$  are the operating temperature and the critical temperature of the superconductor.

In Eq. (1), it is assumed that the magnetic permeability of the (1D-PC) structure is equal to that in free space. Because  $\epsilon_l$  is a periodic function of  $z$ , the dielectric constant can be written as:

$$\epsilon_l(z) = \epsilon_l(z + d) \tag{8}$$

where  $l$  and  $d = d_1 + d_2$  are the number of layer and the period, respectively.

Based on Maxwell’s equations and Boundary conditions, using the boundary conditions and the condition of continuity of  $E$  and  $H$  fields at the interfaces of  $z = 0$  and  $z = d_1, d_2, d_3, \dots, d_{2N}$ , we can find out the relationship between the fields (1D-PC) structure consisting of  $l$  layer; this relation is already exposed by [26, 27]:

$$\begin{bmatrix} E_1 \\ H_1 \end{bmatrix} = M_1 M_2 \dots M_N \dots M_{2N} \begin{bmatrix} E_1 \\ H_1 \end{bmatrix} \tag{9}$$

The matrix  $M_{l,l}$  of the  $l^{th}$  layer can be written in the form:

$$M_{(l-1)} = \begin{bmatrix} \cos(\delta_{(l-1)}) & i\gamma_{(l-1)} \sin(\delta_{(l-1)}) \\ i\gamma_{(l-1)}^{-1} \sin(\delta_{(l-1)}) & \cos(\delta_{(l-1)}) \end{bmatrix} \tag{10}$$

$\delta_{(l-1)}$  and  $\gamma_{(l-1)}$  being the matrix parameters as a function of the incident angle of light, the optical constants, and the thickness of the layer are expressed as:

$$\delta_{(l-1)} = k_{(l-1)} \cdot d_{(l-1)} \cdot \cos\theta_{(l-1)} \tag{11}$$

$$\gamma_{(l-1)} = \begin{cases} \frac{\eta_{(l-1)}}{\cos\theta_{(l-1)}} & \text{TE mode} \\ \eta_{(l-1)} \cos\theta_{(l-1)} & \text{TM mode} \end{cases} \tag{12}$$

where the wave numbers and intrinsic impedances are:

$$k_l = \omega \sqrt{\epsilon_0 \mu_0 \epsilon_l \mu_l} \tag{13}$$

$$\eta_l = \frac{k_l}{\omega \epsilon_l \epsilon_0} = \sqrt{\frac{\mu_0 \mu_l}{\epsilon_0 \epsilon_l}} \tag{14}$$

where  $\epsilon_0, \mu_0, \epsilon_l$ , and  $\mu_l$  are the free space permittivity, free space permeability, relative permittivity, and relative permeability ( $\mu_l = l$ ), respectively.

The  $\theta_{(l-1)}$  is related to the angle of incidence  $\theta_i$  by the SNELL-DESCART law equation:

$$n_{(l-1)} \sin\theta_{(l-1)} = n_0 \sin\theta_0 \tag{15}$$

Considering the transmission matrix of each layer, we can obtain the transmission matrix of the entire structure. For  $l$  number of multilayer’s, the corresponding transfer matrix can be defined as a product of matrices and is obtained from the symmetric PBG structure:

$$M = \prod_{k=1}^{(2N)} M_k = \begin{bmatrix} m_{11} & m_{12} \\ m_{21} & m_{22} \end{bmatrix} \tag{16}$$

The designed (1D-PC) structure with defect layer is depicted in Fig. 2. Here, the host asymmetry (1D-PC) structure with the configuration (Air/(PS)<sup>N/2</sup> D<sub>1</sub> (PS)<sup>N/2</sup>/Air) is made up of MCP (P), superconductor (S), and dielectric materials (D<sub>1</sub>). The product of matrices of (1D-PC) structure with defect layer can be then written as follows [24]:

**Table 1** Photonic band gap, resonant, and cutoff frequency of transmission at different values of the superconductor layer thickness for (Air/(PS)<sup>7</sup> D<sub>1</sub> (PS)<sup>7</sup>/Air) configuration

$d_s$ (nm)	Cutoff frequency [GHz]	Resonant frequency (peak position) [GHz]	Photonic band gap (PBG) [GHz]
40	5.014	13.081	14.992
60	6.673	13.323	16.302
80	7.844	13.562	17.184
100	8.613	13.821	18.221

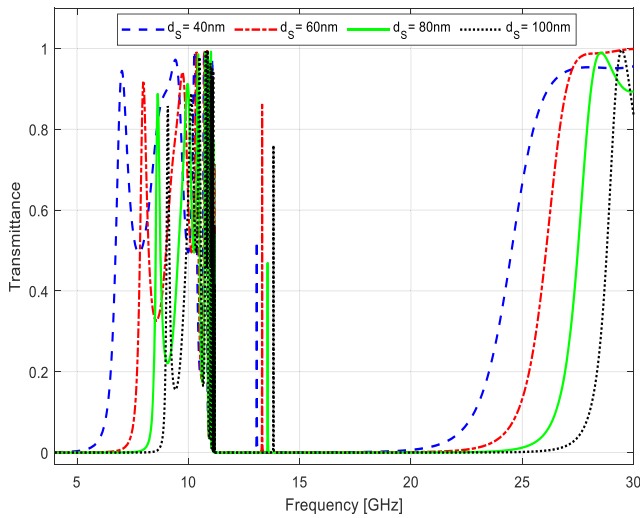


**Fig. 3** The transmission spectra versus the frequency at different values of the superconductor layer thickness. (Air/(PS)<sup>7</sup> D<sub>1</sub> (PS)<sup>7</sup>/Air) θ = 0, (n<sub>c</sub>=10<sup>18</sup>m<sup>-3</sup>, B=0.4T), (λ<sub>0</sub>=200nm, T=4.2K, T<sub>C</sub>=92K), (d<sub>p</sub>=1mm, d<sub>D1</sub>=2mm, n<sub>D1</sub>=2.437)

$$M = \prod_{k=1}^{(2N+1)} M_k = (M_P M_S)^N M_{D1} (M_P M_S)^{(2N+1)}$$

$$= \begin{bmatrix} m_{11} & m_{12} \\ m_{21} & m_{22} \end{bmatrix} \tag{17}$$

where M<sub>P</sub>, M<sub>S</sub>, and M<sub>D1</sub> are the transfer matrixes of the MCP, superconductor, and the defect dielectric layer. m<sub>11</sub>, m<sub>12</sub>, m<sub>21</sub>, and m<sub>22</sub> are the complex numbers.

The transmittance *t* and reflectance *r* are defined as the ratios of the fluxes of the transmitted and reflected waves,

respectively, to the flux of the incident wave. After a few derivations, the total reflection and transmission coefficients are given by [28]:

$$r = \frac{(m_{11} + p_s^{-1} m_{12}) p_0^{-1} - (m_{21} + p_s^{-1} m_{22})}{(m_{11} + p_s^{-1} m_{12}) p_0^{-1} + (m_{21} + p_s^{-1} m_{22})} \tag{18}$$

$$t = \frac{2 \cdot p_0^{-1}}{(m_{11} + p_s^{-1} m_{12}) p_1^{-1} + (m_{21} + p_s^{-1} m_{22})} \tag{19}$$

Here *p*<sub>0</sub> and *p*<sub>s</sub> are the first and last medium of the structure which are given by:

$$p_s^{-1} = \begin{cases} \frac{\eta_s \cos \theta_s}{Z_0} & \text{TE mode} \\ \frac{Z_0}{\eta_s} & \text{TM mode} \end{cases} \tag{20}$$

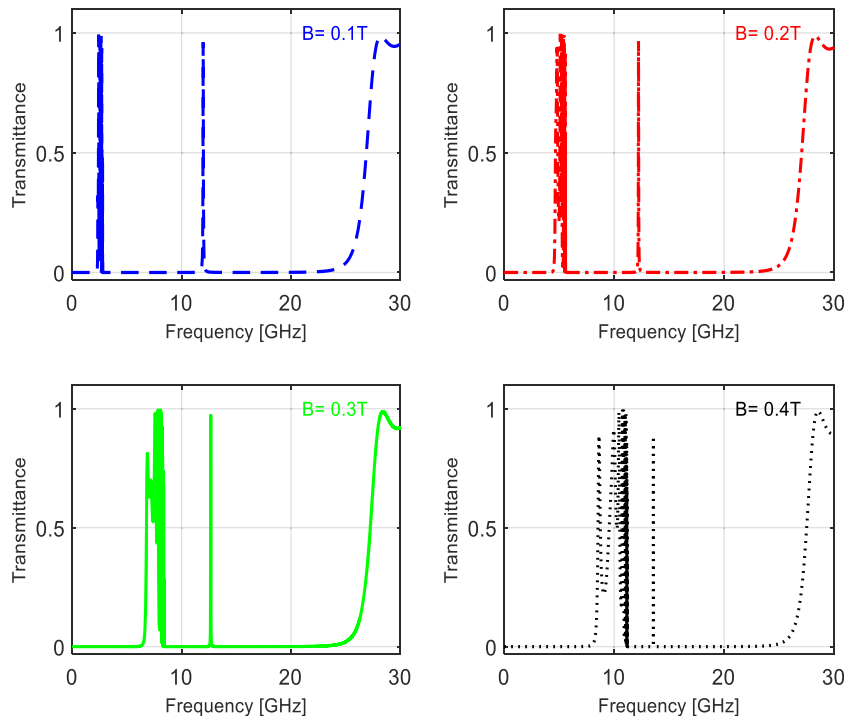
$$p_0^{-1} = \begin{cases} \frac{\eta_0 \cos \theta_0}{Z_0} & \text{TE mode} \\ \frac{Z_0}{\eta_0} & \text{TM mode} \end{cases} \tag{21}$$

where  $Z_0 = \sqrt{\mu_0 / \epsilon_0}$ .

### 3 Numerical Results

In order to check the validity of the method described in section 2, the obtained results for the transmission spectra, the cutoff frequency, and the peak position as function of the different parameters values of one-dimensional defective

**Fig. 4** Transmission spectra versus frequency with variation of external magnetic field. (Air/(PS)<sup>7</sup> D<sub>1</sub> (PS)<sup>7</sup>/Air) θ<sub>0</sub>=0, (n<sub>c</sub>=10<sup>18</sup>m<sup>-3</sup>, (λ<sub>0</sub>=200nm, T=4.2K, T<sub>C</sub>=92K), (d<sub>p</sub>=1mm, d<sub>S</sub>=80nm, d<sub>D1</sub>=2mm, n<sub>D1</sub>=2.437)



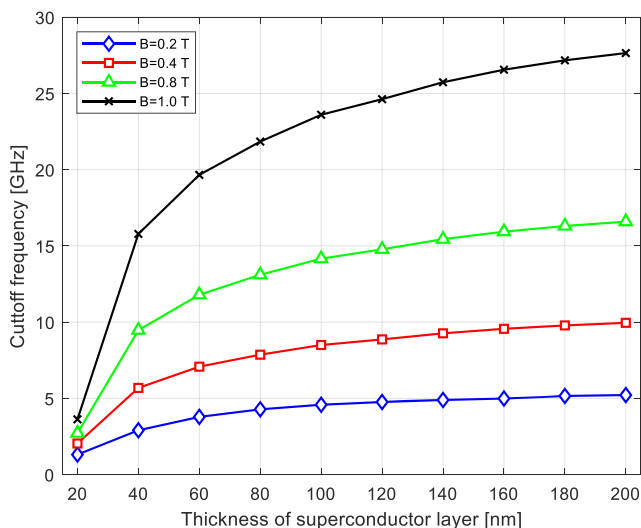


**Fig. 5** The cutoff frequency of 1D defective PCs versus the thickness of the superconductor layer at different values of magnetic field

photonic crystal structure, containing the magnetized cold plasma and high temperature superconductor layer, have been investigated. The proposed structure is restructured as Air/(P<sub>n</sub>S<sub>n</sub>)<sup>n</sup> D<sub>1</sub> (P<sub>n</sub>S<sub>n</sub>)<sup>n</sup>/Air, where n = 1...N/2 and N is chosen as 14. The MCP material (P<sub>n</sub>) parameters to be used in the following calculations are n<sub>c</sub> = 10<sup>18</sup> m<sup>-3</sup> [17], γ = 2 × (2π) × 10<sup>4</sup> Hz [19], and d<sub>p</sub> = 1 mm. For the superconducting layers (S<sub>n</sub>) we use YBa<sub>2</sub>Cu<sub>3</sub>O<sub>7</sub>. With critical temperature T<sub>C</sub> = 92 K, penetration depth at T = 0 K is λ<sub>0</sub> = 200 nm, the operating temperature is (T = 4.2 K) and n<sub>sup</sub> = n<sub>YBa2Cu3O7</sub> = √ε<sub>S</sub> = √[1 - (ω<sub>th</sub>/ω)<sup>2</sup>] [20]. The Titanate de strontium SrTiO<sub>3</sub> is a material of the first defective layer (D<sub>1</sub>) with refractive index n<sub>D1</sub> = 2.437 [29] and thickness d<sub>D1</sub> = 2 mm, also we choose the Indium Arsenide InAs as second defective layer (D<sub>2</sub>) with n<sub>D2</sub> = n<sub>InAs</sub> = 3.384 [29] and thickness d<sub>D2</sub> = 2 mm.

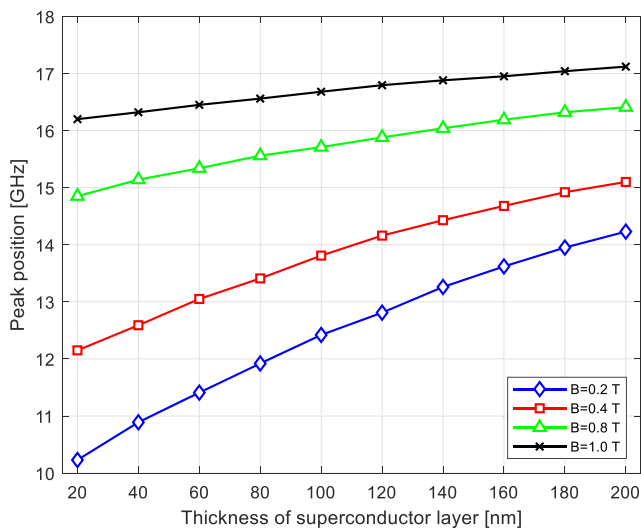


**Fig. 6** The peak position of 1D defective PCs versus the thickness of the superconductor layer at different values of magnetic field

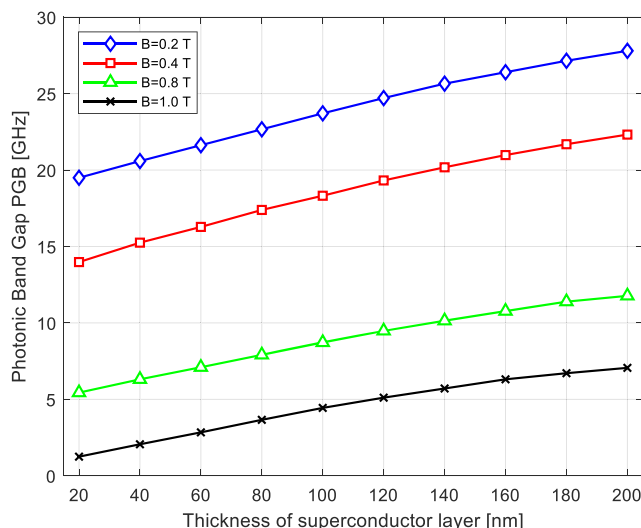


**Fig. 7** The photonic band gap versus the thickness of the superconductor layer at different values of magnetic field

### 3.1 The Superconductor Thickness Effect on the Transmittance Spectra

Figure 3 shows the transmission spectra versus the frequency for four different values of the superconductor material thickness. The dimension of the superconductor layer is chosen to be d<sub>s</sub> = 40, 60, 80, and 100 nm, where the thickness of MCP layer and the defect layer remained unchanged. From the Fig. 3, when the frequency belongs to the interval [5 8.5] GHz, the width of photonic band gap is more sensitive to the increasing of superconductor layer’s thickness. In addition, when d<sub>s</sub> = 40 nm, the appearance of the cutoff frequency (f<sub>c</sub>) at 5.014 GHz, for frequencies less than f<sub>c</sub>, we see that the appearance of the PBG. It is clear that further increases in the values of d<sub>s</sub> to 60, 80, and 100 nm

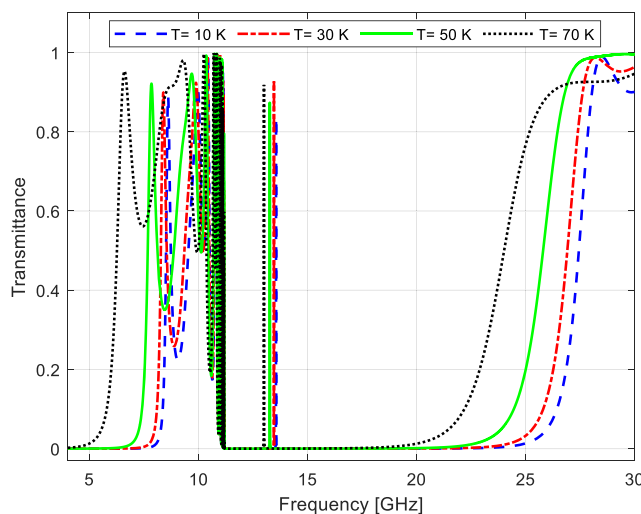


**Fig. 8** The transmission spectra versus the frequency at different values of temperature. (Air/(PS)<sup>7</sup> D<sub>1</sub> (PS)<sup>7</sup>/Air) θ=0, (n<sub>c</sub>=10<sup>18</sup>m<sup>-3</sup>, B=0.4T), (λ<sub>0</sub>=200nm, T<sub>C</sub>=92K), (d<sub>p</sub>=1mm, d<sub>s</sub>=80nm, d<sub>D1</sub>=2mm, n<sub>D1</sub>=2.437)

**Table 2** Photonic band gap, resonant, and cutoff frequency of transmission for different values of the temperature for (Air/(PS)<sup>7</sup> D<sub>1</sub> (PS)<sup>7</sup>/Air) configuration

T (K)	Cutoff frequency [GHz]	Resonant frequency (peak position) [GHz]	Photonic band gap (PBG) [GHz]
10	7.770	13.560	17.240
30	7.395	13.450	16.870
50	6.491	13.270	16.670
70	4.265	13,000	15.470

lead to a significant increase in the value of the cutoff frequency (6.673, 7.844, and 8.613 GHz). In other words, the cutoff frequency shifts towards higher frequency regions with increasing the superconductor layer thickness. Apropos of *frequency interval* [13–14] GHz, we notice the appearance of the resonant frequency 13.08 GHz when  $d_S = 40$  nm, 13.32 GHz when  $d_S = 60$  nm, 13.56 GHz when  $d_S = 80$  nm, and 13.82 GHz when  $d_S = 100$  nm. Finally, we conclude that the superconductor thickness is a significant parameter in this structure Table 1.

### 3.2 External Magnetic Field Effect on the Transmittance Spectra

In this part, we investigate the influence of the external magnetic field on transmission spectra, cutoff frequency, photonic band gap, and peak position. From the results of Fig. 4, it is found that a small displacement of the default peak position. When increasing the external electric field  $B$ , photonic band gap decreases, and more ripple appears at the cutoff frequency, which shifts to the left.

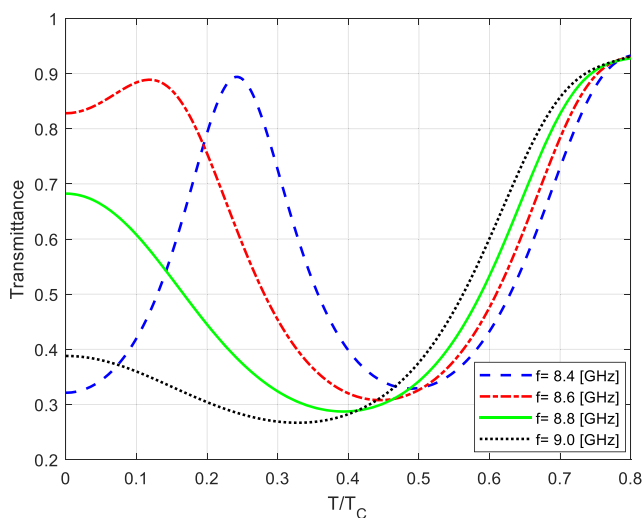


**Fig. 9** The transmission spectra versus the temperature at different frequencies. (Air/(PS)<sup>7</sup> D<sub>1</sub> (PS)<sup>7</sup>/Air)  $\theta_0=0$ , ( $n_c=10^{18}\text{m}^{-3}$ ,  $B=0.4\text{T}$ ), ( $\lambda_0=200\text{nm}$ ,  $T_C=92\text{K}$ ), ( $d_p=1\text{mm}$ ,  $d_S=80\text{nm}$ ,  $d_{D1}=2\text{mm}$ ,  $n_{D1}=2.437$ )

### 3.3 Effect of the External Magnetic Field and the Thickness of the Superconductor Layer on the Transmittance Spectra

In order to observe the effect of the thickness of the superconductor layer and the external magnetic field on the cutoff frequency, peak position, and the photonic band gap, we vary the external magnetic field from 0.2 to 1 T and 20 to 200 nm. From the results of Fig. 5, it can be seen that the effect of varying the thickness of the superconductor layer on the cutoff frequency is significant only for value near the 200 nm. Figure 6 shows that the peak position increase with the increase in the thickness of superconductor layer and magnetic field and shifts towards the higher frequency regions. Fig. 7 shows the photonic band gap of the defective 1D PC structure as a function of the thickness of the superconducting layer, by varying the magnetic field. The PBG increases with the increase in the thickness of superconductor layer and decreases with the increase in the external magnetic field and shifts towards the higher frequency regions.

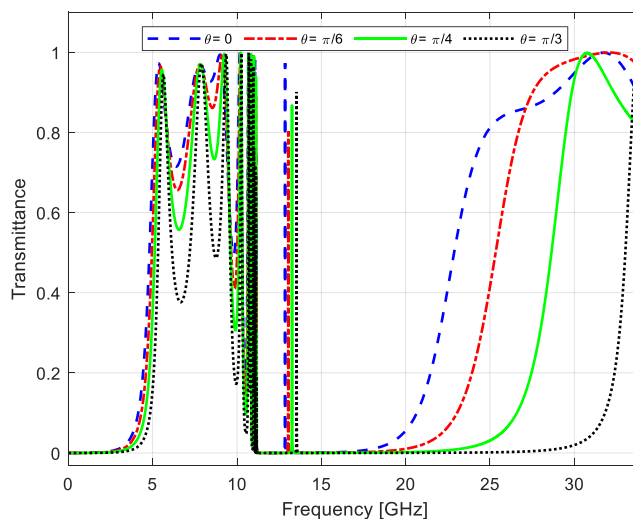


**Fig. 10** Transmission spectra versus frequency with variation of incident angle for TE mode. (Air/(PS)<sup>7</sup> D<sub>1</sub> (PS)<sup>7</sup>/Air), ( $n_c=10^{18}\text{m}^{-3}$ ,  $B=0.4\text{T}$ ), ( $\lambda_0=200\text{nm}$ ,  $T=4.2\text{K}$ ,  $T_C=92\text{K}$ ), ( $d_p=1\text{mm}$ ,  $d_S=20\text{nm}$ ,  $d_{D1}=2\text{mm}$ ,  $n_{D1}=2.437$ )

**Table 3** Photonic band gap, resonant, and cutoff frequency of transmission at different values of incident angle TE mode, for (Air/(PS)<sup>7</sup>D<sub>1</sub>(PS)<sup>7</sup>/Air) configuration

$\theta$ (rad)	Cutoff frequency [GHz]	Resonant frequency (peak position) [GHz]	Photonic band gap (PBG) [GHz]
0	2.280	12.85	13.85
$\pi/6$	2.533	13.04	16.71
$\pi/4$	2.791	13.26	19.47
$\pi/3$	3.233	13.53	22.67

### 3.4 Temperature Effect on the Transmittance Spectra

In Fig. 8, results are presented for the transmittance spectra of the structure (Air/(PS)<sup>7</sup>D<sub>1</sub>(PS)<sup>7</sup>/Air) versus the variation in the frequency for several temperature. It can be observed that increasing the temperature will decrease the cutoff frequency. This reduction is significant for temperatures near the 70 K. Also, it is found that the peak position of the defective structure shifts towards low temperatures. The same behavior has found theoretically for the case of 1D magnetized cold plasma-high T<sub>C</sub> superconductor PC (without the defect) [20, 30], which showed that the cutoff frequency decreases with increasing temperature. In Table 2, we present the calculated results of the cutoff frequency, the resonant frequency, and the photonic band gap at different values of temperature.

In addition, Fig. 9 illustrates the variation of the transmittance as a function of the temperature at frequencies 8.4 to 9.0 GHz higher than cutoff frequency. At high temperature, a strong oscillation is seen, while the oscillation in transmittance is weak [20, 30]. In other words, the PBG band can be adjusted by varying the temperature. The structure is therefore temperature dependent which could be useful in superconducting electronics.

### 3.5 Incident Angle Effect on the Transmittance Spectra

Figure 10 and Table 3 show theoretical effects of the variation of angle of incidence and frequency on the transmittance spectra for TE mode. It is interesting to note that for the TE

polarization, we have found acceptable results for the filter application, but for the application of TM, poor results are obtained. These changes can be attributed to polarization effects and increased mismatch in the optical thickness of adjacent layers.

### 3.6 The Resonant Structures and Quality Factor Q

The trends of variation of the resonant frequencies, the width of the photonic band gap and the quality factor are also presented. For the resonant structures, we notice that the ability is expressed in terms of quality factor Q [29], where  $Q = f_r/\Delta f$ ,  $f_r$  is resonance frequency, and  $\Delta f$  is the line width of the resonance peak. The quality factor therefore makes it possible to quantify the “quality of a filter,” higher Q, more selective filter. The resonant peak is located at the design frequency of  $f_r = 13.566$  GHz with quality factor values of  $Q = 7140$ , for the (Air/(PS)<sup>7</sup>D<sub>1</sub>(PS)<sup>7</sup>/Air).

To investigate the relationship between the number of defect layers and defect modes, we have plotted the transmission spectra depending on the frequency. The refractive indices of defect layers were selected:  $n_{D1} = n_{SrTiO3} = 2.437$  and  $n_{D2} = n_{InAs} = 3.3842$  [29].

In Fig. 11, we have plotted the transmission spectra of the asymmetric (1D-PC) structure with the configuration (Air/(PS)<sup>7</sup>D<sub>2</sub>SD<sub>1</sub>(PS)<sup>7</sup>/Air). In addition, we can observe from Fig. 12 that the (1D-PC) structure with the configuration (Air/(PS)<sup>7</sup>D<sub>1</sub>PD<sub>1</sub>SD<sub>1</sub>(PS)<sup>7</sup>/Air) with  $n_{D1} = n_{SrTiO3} = 2.437$  shows the existence three defect modes respectively within the photonic band gap (PBG).The resonant peak is

**Table 4** Frequency of transmission peak and quality factor Q for different configurations

Configuration	Peaks	$f_r$ [GHz]	$\Delta f$ [GHz]	$Q=f_r/\Delta f$
(Air/(PS) <sup>7</sup> D <sub>1</sub> (PS) <sup>7</sup> /Air)	1 <sup>st</sup> peak	13.566	0.0019	7140.00
(Air/(PS) <sup>7</sup> D <sub>2</sub> SD <sub>1</sub> (PS) <sup>7</sup> /Air)	1 <sup>st</sup> peak	8.173	0.0015	5448.67
	2 <sup>nd</sup> peak	16.241	0.03	541.33
(Air/(PS) <sup>7</sup> D <sub>1</sub> PD <sub>1</sub> SD <sub>1</sub> (PS) <sup>7</sup> /Air)	1 <sup>st</sup> peak	8.028	0.0016	5017.50
	2 <sup>nd</sup> peak	13.181	0.0041	3214.63
	3 <sup>rd</sup> peak	19.811	0.06	330.17

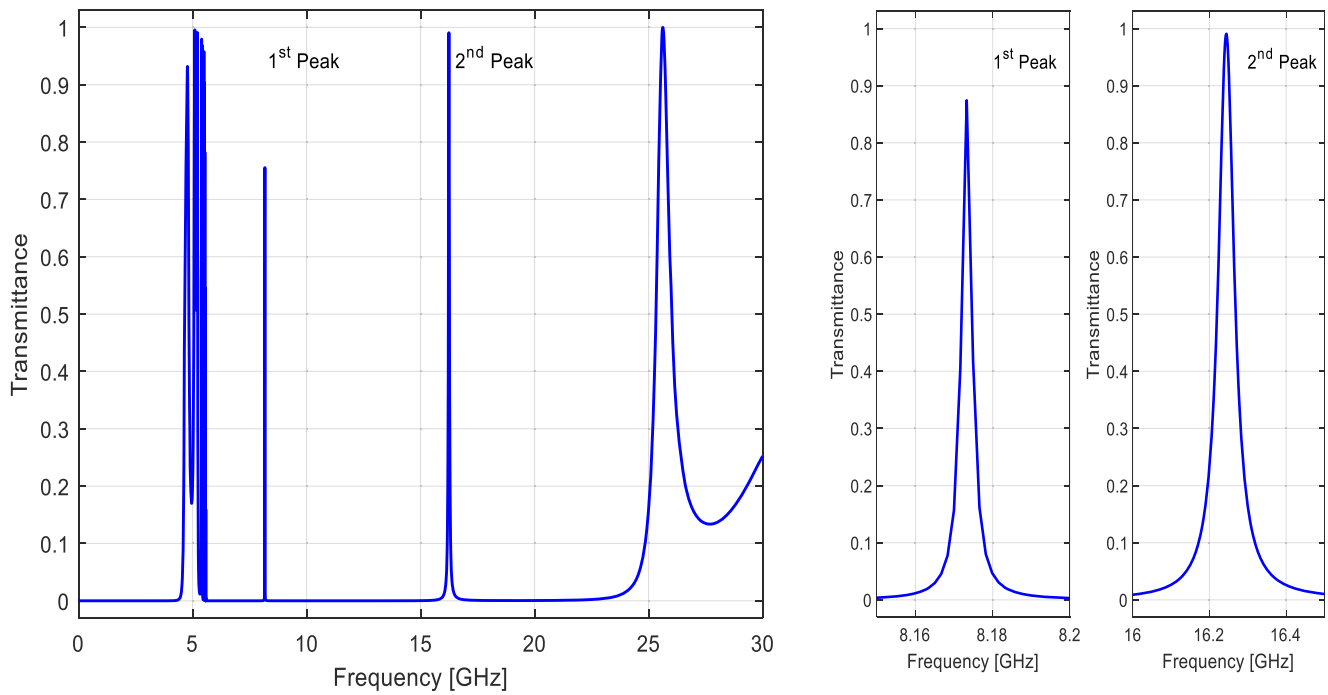


**Fig. 11** Transmission spectra of  $(\text{Air}/(\text{PS})^7 \text{D}_2\text{SD}_1 (\text{PS})^7/\text{Air})$  configuration calculated as a function of frequency.  $n_{\text{D1}}=n_{\text{SrTiO}_3}=2.437$ ,  $n_{\text{D2}}=n_{\text{InAs}}=3.3842$ ,  $d_p=1\text{mm}$ ,  $d_s=80\text{nm}$ ,  $d_{\text{D1}}=d_{\text{D2}}=2\text{mm}$ ,  $B=0.2\text{T}$ ,  $n_e=10^{18}\text{m}^{-3}$

located at the design frequency of ( $f_{r1} = 8.173$  GHz,  $f_{r2} = 16.241$  GHz) with quality factor values of ( $Q_1 = 5448.67$ ,  $Q_2 = 541.33$ ), for the  $(\text{Air}/(\text{PS})^7 \text{D}_2\text{SD}_1 (\text{PS})^7/\text{Air})$  configuration and ( $f_{r1} = 8.028$  GHz,  $f_{r2} = 13.181$  GHz,  $f_{r3} = 19.811$  GHz) and ( $Q_1 = 5017.50$ ,  $Q_2 = 3214.63$ ,  $Q_3 = 330.17$ ) for

$(\text{Air}/(\text{PS})^7 \text{D}_1\text{PD}_1\text{SD}_1 (\text{PS})^7/\text{Air})$  configuration. Our results imply that the number of defect mode can be increased by the adding of defect layers in structure Table 4.

The results for the quality factors as a function of external magnetic field are plotted in Fig. 13. The dependences of the

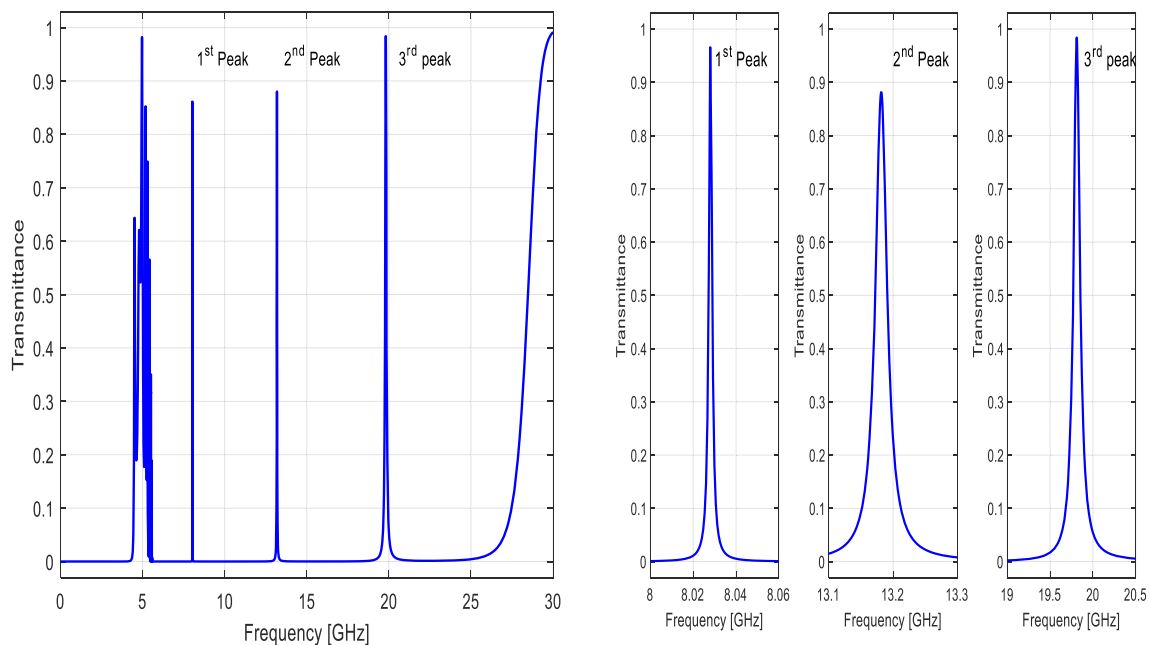
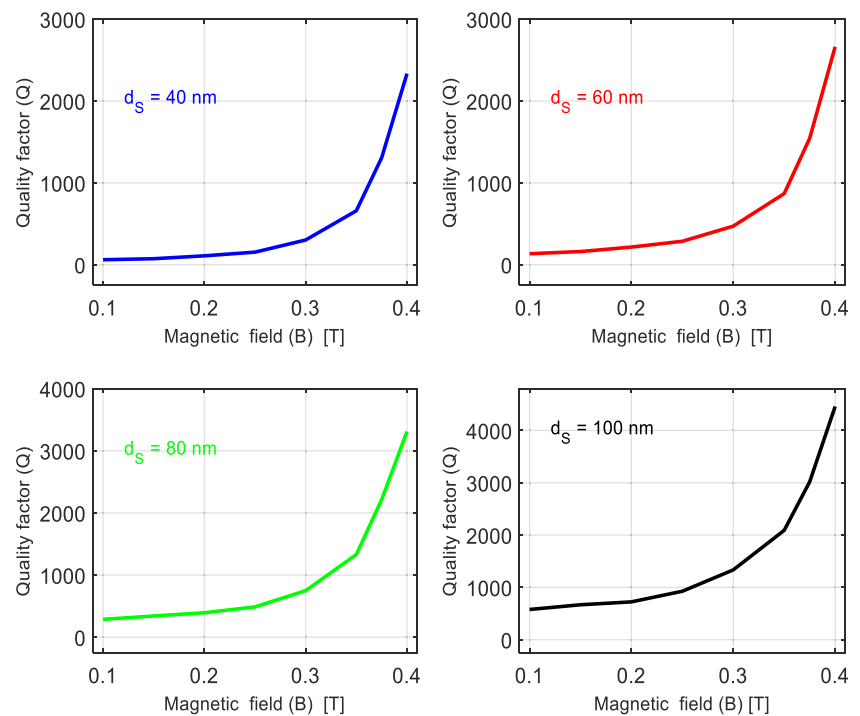


**Fig. 12** Transmission spectra of  $(\text{Air}/(\text{PS})^7 \text{D}_1\text{PD}_1\text{SD}_1 (\text{PS})^7/\text{Air})$  configuration calculated as a function of frequency.  $n_{\text{D1}}=n_{\text{SrTiO}_3}=2.437$ ,  $d_p=1\text{mm}$ ,  $d_s=80\text{nm}$ ,  $d_{\text{D1}}=2\text{mm}$ ,  $B=0.2\text{T}$ ,  $n_e=10^{18}\text{m}^{-3}$



**Fig. 13** Variation of quality factor as a function of the external magnetic field for different thickness of the superconductor layer. Structure (Air/(PS)<sup>7</sup> D<sub>1</sub> (PS)<sup>7</sup>/Air). TE mode,  $\theta_0 = 0$ , ( $n_e = 10^{18} \text{ m}^{-3}$ ,  $d_p = 1 \text{ mm}$ ), ( $\lambda_0 = 200 \text{ nm}$ ,  $T = 4.2 \text{ K}$ ,  $T_C = 92 \text{ K}$ ), ( $d_{D1} = 2 \text{ mm}$ ,  $n_{D1} = 2.437$ )



quality factor at the resonant mode on the magnetic field strength show the high transmission and the maximum Q factor appears at  $B=0.4 \text{ T}$  for different thickness of the superconductor layer. The existence of the resonant mode is intuitive, that is, by coupling the downshifted waves and trapping of an electromagnetic wave. We have also indicated that using high temperature superconductors (HTS) layer of the thickness about  $100 \text{ nm}$  has offset the usual reduction in performance with miniaturization. This miniaturization not only produces the microwave filter smaller but also reduces the cooling systems of superconductor.

## 4 Conclusion

In this work, a new design and analysis of one-dimensional defective photonic crystal structure, containing the magnetized cold plasma and high temperature superconductor layer, are presented. Theoretical results in terms of the transmission spectra for the various (1D-PCs) configurations were presented and theoretically investigated by the transfer matrix method (TMM). Current simulations show that the width of the photonic band gap can be adjusted by modifying superconductor layer's thickness and the magnetic field. In case of fixed temperature, increasing the superconductor layer's thickness, also magnetic field could increase the width of the photonic band gap.

Moreover, due to the existence of a defective layer, it is apparently shown that there is a very narrow pass band within the photonic band gap. The number of the defect modes can be controlled by adjusting the number of defect layers in the structure. Therefore, the proposed structure configurations may be of potential use and interest in many applications such as optical communication selective filters. The obtained results have been compared with the published data available in literature and good agreement and correspondence that have been found.

## References

1. Kumar, V., Suthar, B., Kumar, A., Singh, K.S., Bhargava, A., Ojha, S.P.: Silicon based one-dimensional photonic crystal as a TM-mode filter. *Silicon*. **6**, 73–78 (2014)
2. Srivastava, S.K., Aghajamali, A.: Study of optical reflectance properties in 1D annular photonic crystal containing double negative (DNG) metamaterials. *Phys. B Condens. Matter*. **489**, 67–72 (2016)
3. El-Khozondar, H.J., Mahalakshmi, P., El-Khozondar, R.J., Ramanujam, N.R., Amiri, I.S., Yupapin, P.: Design of one dimensional refractive index sensor using ternary photonic crystal waveguide for plasma blood samples applications. *Physica E: Low-Dimen, Syst. Nanostruct.* **111**, 29–36 (2019)
4. Nejad, H.E., Mir, A., Farmani, A.: Supersensitive and tunable nano-biosensor for cancer detection. *IEEE Sensors J.* **19**, 4874–4881 (2019)

5. Soltani, A., Ouerghi, F., AbdelMalek, F., Haxha, S.: Comparative study of one-dimensional photonic crystal heterostructure doped with a high and low-transition temperature superconducting for a low-temperature sensor. *Opt. Commun.* **445**, 268–272 (2019)
6. Nouman, W.M., Abd El-Ghany, S.E.-S., Sallam, S.M., Dawood, A.B., Aly, A.H.: Biophotonic sensor for rapid detection of brain lesions using 1D photonic crystal. *Opt. Quant. Electron.* **52**, 287 (2020)
7. Kumar, V., Suthar, B., Kumar, A., Bhargava, A.: Design of a wavelength division demultiplexer using Si-based one-dimensional photonic crystal with a defect. Elsevier, *Optik*. **124**, 2527–2530 (2013)
8. Aly, A.H., Aghajamali, A.A., Elsayed, H., Mobarak, M.: Analysis of cutoff frequency in a one-dimensional superconductor-metamaterial photonic crystal. *Physica C: Supercond Appl.* **528**, 5–8 (2016)
9. Aly, A.H., Mohamed, D.: The Optical Properties of Metamaterial-Superconductor Photonic Band Gap With/Without Defect Layer. *J. Supercond. Nov. Magn.* **32**, 1897–1902 (2018)
10. Aly, A.H., Ameen, A.A., Elsayed, H.A., Mohamed, S.H., Singh, M.R.: One-dimensional metallo-superconductor photonic crystals as a smart window. *J. Supercond. Nov. Magn.* 1–6 (2019)
11. Zaky, Z.A., Aly, A.H.: Theoretical study of a tunable low-temperature photonic crystal sensor using dielectric-superconductor nanocomposite layers. *J. Supercond. Nov. Magn.* **33**, 2983–2990 (2020)
12. Hojo, H., Mase, A.: Electromagnetic-wave transmittance characteristics in one-dimensional plasma photonic crystals. *J. Plasma Fusion Res. Ser.* **8**, 477–479 (2009)
13. Guo, B.: Photonic band gap structures of obliquely incident electromagnetic wave propagation in a one-dimension absorptive plasma photonic crystal. *Phys. Plasmas.* **16**(043508), 1–6 (2009)
14. Fan, W., Dong, L.: Tunable one-dimensional plasma photonic crystals in dielectric barrier discharge. *Phys. Plasmas.* **17**, 1–6 (2010)
15. Qi, L.: The absorbing properties of one-dimensional plasma photonic crystals. *Aust. J. Plant Physiol.* **82**(1), (2016)
16. Abadla, M.M., Tabaza, N.A., Tabaza, W., Ramanujam, N.R., Joseph Wilson, K.S., Vigneswaran, D., Taya, S.A.: Properties of ternary photonic crystal consisting of dielectric/plasma/dielectric as a lattice period. *Optik*. **185**, 784–793 (2019)
17. Qi, L., Yang, Z., Fu, T.: Defect modes in one-dimensional magnetized plasma photonic crystals with a dielectric defect layer. *Phys. Plasmas.* **19**(1), 012509 (2012)
18. Aly, A.H., Elsayed, H.A., Ameen, A.A., Mohamed, S.H.: Tunable properties of one-dimensional photonic crystals that incorporate a defect layer of a magnetized plasma. *Int. J. Modern Phys. B.* **31**, 1750239 (2017)
19. Chang, T.-W., Chien, J.-R.C., Wu, C.-J.: Magnetic-field tunable multichannel filter in a plasma photonic crystal at microwave frequencies. *Appl. Opt.* **55**, 943–946 (2016)
20. Aghajamali, A.: Transmittance properties in a magnetized cold plasma-superconductor periodic multilayer. *Appl. Opt.* **55**, 6336–6340 (2016)
21. H. G. Booker, *Cold Plasma Waves* (Springer-Verlag, 1984), pp. 23–25.
22. Lee, H.M., Wu, J.C.: Transmittance spectra in one-dimensional superconductor-dielectric photonic crystal. *J. Appl. Phys.* **107**, 09E149–09E149-3 (2010)
23. Hu, C.-A., Liu, J.-W., Wu, C.-J., Yang, T.-J., Yang, S.-L.: Effects of superconducting film on the defect mode in dielectric photonic crystal heterostructure. *Solid State Commun.* **157**, 54–57 (2013)
24. Aly, A. H., Sabra, W., Abdel-Rahman, E.: Investigation of the transmittance in superconducting photonic crystal. *Progress In Electromagnetics Research Symposium Proceedings, KL, MALAYSIA, March 27-30* (2012)
25. Aly, A.H.: Metallic and superconducting photonic crystal. *J. Supercond. Nov. Magn.* **21**, 421–425 (2008)
26. Scotognella, F.: Four-material one dimensional photonic crystals. *Opt. Mater.* **34**, 1610–1613 (2012)
27. Oraizi, H., Abdolali, A.: Several theorems for reflection and transmission coefficients of plane wave incidence on planar multilayer metamaterial structures. *IET Microw. Antennas Propag.* **4**, 1870–1879 (2010)
28. Wu, C.-J.: Transmission and reflection in a periodic superconductor/dielectric film multilayer structure. *J. Electromagnet Waves Appl.* **19**, 1991–1996 (2005)
29. Mamri, B., Barkat, O.: Design of a selective filter based on one-dimensional superconductor photonic crystal. *J. Supercond. Nov. Magn.* **32**, 3397–3405 (2019)
30. Aly, A.H., Ryu, S.-W., Hsu, H.-T., Wu, C.-J.: THz transmittance in one-dimensional superconducting nanomaterial-dielectric superlattice. *Mater. Chem. Phys.* **113**, 382–384 (2009)

**Publisher's note** Springer Nature remains neutral with regard to jurisdictional claims in published maps and institutional affiliations.